European Radiology (2019) 29:4357–4367
https://doi.org/10.1007/s00330-018-5956-3

CARDIAC

Comprehensive evaluation of macroscopic and microscopic myocardial fibrosis by cardiac MR: intra-individual comparison of gadobutrol versus gadoterate meglumine

Amir Ali Rahsepar[1,2] · Ahmadreza Ghasemiesfe[1,2] · Kenichiro Suwa[1] · Ryan S. Dolan[1] · Monda L. Shehata[1] · Monica J. Korell[1] · Nivedita K. Naresh[1] · Michael Markl[1] · Jeremy D. Collins[1,3] · James C. Carr[1]

Received: 22 August 2018 / Revised: 14 November 2018 / Accepted: 5 December 2018 / Published online: 7 January 2019

Abstract

Purpose Late gadolinium enhancement cardiac MR (LGE-CMR) and extracellular volume fraction (ECV-CMR) are widely used to evaluate macroscopic and microscopic myocardial fibrosis. Macrocyclic contrast media are increasingly used off-label for myocardial scar assessment, given the superior safety profile of these agents. We aimed to assess the performance of two macrocyclic contrast agents, gadoterate meglumine and gadobutrol, for the evaluation of myocardial scar.

Material and methods Forty subjects (61 ± 11 years, 67.5% men) who underwent LGE-CMR using gadobutrol were prospectively recruited for a research CMR scan using same-dose gadoterate meglumine (0.2 mmol/kg) at 1.5 T. Myocardial scar quantification was performed using a short-axis phase-sensitive inversion recovery (PSIR) Turbo-FLASH and steady-state free precession (SSFP) images. Pre- and post-contrast T1-mapping was employed to assess myocardial ECV. An intraclass correlation coefficient (ICC) was used to check for reliability between the two contrast agents.

Results Using manual thresholding on PSIR Turbo-FLASH images, mean LGE scar percentage (LGE%) was 9.9 ± 9.7% and 9.4 ± 9.7% for gadobutrol and gadoterate meglumine, respectively ($p > 0.05$) (ICC: 0.99, 95% CI: 0.97–0.99). Using the PSIR SSFP technique and manual thresholding, LGE% averaged 7.5 ± 9.0% and 7.1 ± 8.6% for gadobutrol and gadoterate meglumine, respectively ($p > 0.05$) (ICC: 0.99, 95% CI: 0.98–0.99). Average ECV with gadobutrol and gadoterate meglumine were similar at 28.40 ± 4.88 and 28.46 ± 4.73 ($p > 0.05$) with a strong correlation (ICC: 0.98, 95% CI: 0.94–0.99).

Conclusion We found LGE- and ECV-CMR values derived from gadoterate meglumine comparable to values derived from gadobutrol. Gadoterate meglumine has a comparable performance to gadobutrol in identifying LGE-derived myocardial scar both qualitatively and quantitatively.

Key Points

- *Late gadolinium-enhancement cardiac MR (LGE-MR) and extracellular volume (ECV) fraction are widely used to evaluate macroscopic and microscopic myocardial fibrosis.*
- *Macrocyclic contrast media are increasingly used off-label for myocardial scar assessment, given the presumed superior safety profile of these agents.*
- *LGE- and ECV-CMR values derived from gadoterate meglumine are comparable to values derived from gadobutrol.*

Keywords Heart · Magnetic resonance imaging · Contrast agents · Scar

✉ Amir Ali Rahsepar
amir.rahsepar@northwestern.edu

[1] Department of Radiology, Feinberg School of Medicine, Northwestern University, 737 N. Michigan Ave., Suite 1600, Chicago, IL 60611, USA

[2] Department of Radiology, Yale New Haven Health, Bridgeport Hospital, Bridgeport, CT, USA

[3] Department of Radiology, Mayo Clinic, Rochester, MN, USA

Abbreviations

CI	Confidence interval
CMR	Cardiac magnetic resonance
CNR	Contrast-to-noise ratio
ECV	Extracellular volume
GBCA	Gadolinium-based contrast agents
GFR	Glomerular filtration rate
ICC	Intraclass correlation coefficients
LGE	Late gadolinium enhancement

LV	Left ventricle
MOLLI	Modified Look-Locker inversion recovery
PSIR	Phase-sensitive inversion recovery
SI	Signal intensity
SNR	Signal-to-noise ratio
SSFP	Steady-state free precession

Introduction

Cardiac MRI provides high tissue contrast and spatial resolution and is the reference standard for evaluation of myocardial structure [1]. Late gadolinium enhancement cardiac magnetic resonance (LGE-CMR) imaging is a reference standard for myocardial scar evaluation [2, 3] and can help to identify and characterize scar in both non-ischemic and ischemic cardiomyopathies [4, 5], enabling risk stratification and clinical management.

While LGE can effectively detect dense focal myocardial fibrosis at the macroscopic level, it is ineffective in the identification of diffuse interstitial fibrosis [6]. In cardiomyopathies with infiltrative and reactive interstitial fibrosis, T1-mapping has proven to be useful to accurately detect diffuse myocardial fibrosis [7]. Moreover, post-gadolinium contrast T1 times, along with native (pre-contrast) T1 times, are used to derive the myocardial extracellular volume (ECV) [8]. ECV is calculated using pre-and post-contrast T1 values, the left ventricular (LV) blood pool, and the patient's hematocrit. The application of T1-mapping and ECV has shown promise in the identification of different disease processes related to the development of myocardial fibrosis [9].

Gadolinium-based contrast agents (GBCA) used for LGE- and ECV-CMR evaluation are subdivided into linear and macrocyclic chelates based on their chemical structure. LGE-CMR was originally described using linear GBCAs, but recent reports have demonstrated that serial application of linear GBCAs is associated with increased gadolinium deposition in extravascular tissues, most notably cerebral tissue, independent of renal function [10–12], causing a gradual shift in practice towards increased use of macrocyclic GBCAs due to their presumed superior safety profiles. As previously reviewed [13], a higher kinetic stability of macrocyclic structure in combination with a high thermodynamic stability can decrease the amount of free gadolinium released in the body. However, it is not clear that all macrocyclic agents with their slightly different chemical structures and characteristics, such as relaxivity, act in exactly the same way and can be used interchangeably. Due to the recent introduction of gadoterate meglumine to the US market, and the crucial role of myocardial fibrosis detection by CMR, we aimed to assess LGE- and ECV-CMR using the recently introduced macrocyclic GBCA, gadoterate meglumine (Dotarem, Guerbet), and compare it to gadobutrol (Gadavist [US name]/Gadovist [European name], Bayer).

Patients and methods

Study population

More than 500 subjects who were referred for LGE-CMR using standard of care 0.2 mmol/kg gadobutrol to evaluate for cardiomyopathy and were suspicious of having myocardial scar were approached and invited to participate in the study. Out of these 500 patients, 40 were prospectively recruited to undergo an additional research CMR scan using 0.2 mmol/kg gadoterate meglumine. All research scans were scheduled within 8 weeks (range 2–8 weeks) of the original clinically indicated CMR using gadobutrol. All subjects aged between 18 and 89 years and had a glomerular filtration rate (GFR) ≥ 60 mL/min/1.73 m^2, as measured within 24 h of each scan. Subjects who developed any contraindication to MRI (e.g., new implantable device) between the clinical and research exams were excluded. This study was approved by an institutional review board, and written informed consent was obtained from all subjects. Immediately assessable adverse events were included.

Magnetic resonance imaging protocol

All scans were performed on 1.5-Tesla MR scanners (MAGNETOM Avanto/Aera, Siemens Healthcare). Images were acquired in sequential short-axis slices from the atrioventricular annulus to the LV apex. At 7–10 min following 0.2 mmol/kg contrast injection, a series of free-breathing short-axis and long-axis (2-, 3-, and 4-chamber) images were acquired using an SSFP-based phase-sensitive inversion recovery (PSIR) pulse sequence (PSIR SSFP) (slice thickness: 6 mm, gap 2 mm, pixel spacing = 2–2.2 × 2–2.2 mm^2, TE 1.2 ms, TR 960 ms). Following the PSIR SSFP image acquisition, breath-held LGE imaging was performed using a segmented PSIR Turbo-FLASH pulse sequence (pixel spacing = 1.3–1.6 × 1.3–1.6 mm^2, slice thickness 6 mm, and gap 4 mm, TE 3.3 ms, TR 500–860 ms). Parallel imaging with GRAPPA was used for both SSFP and Turbo-FLASH techniques. For both LGE sequences, the inversion time was selected carefully to optimally null normal myocardium, (typical values 260–340 ms) [14]. Image resolution, as well as the time interval between contrast injection and SSFP and Turbo-FLASH image acquisition, was matched between the first and second scans. Each CMR study may have included SSFP and/or Turbo-FLASH images per the institutional imaging protocol customized for each type of CMR studies, and thus, not all subjects had a complete set of SSFP and Turbo-FLASH images. T1-mapping was performed using a modified Look-Locker inversion recovery (MOLLI) technique as described previously [15]. Base, mid, and apical slices were acquired during breath-hold before and 15–25 min following the intravenous administration of the contrast agent bolus.

T1-mapping parameters were as follows: spatial resolution (pixel size) 1–1.4 × 1–1.4 mm^2, slice thickness 8 mm, TE/TR 1.0–1.3 ms/2.0–2.2 ms; flip angle 35°. Patient hematocrit was collected immediately before the cardiac MRI exam.

Image analysis

Quantitative analysis of scar burden

Quantitative assessment of myocardial scar was performed on LGE-CMR data on short-axis images using Circle post-processing software version 5.3 [16]. Quantitative assessment was performed by two physicians (A.A.R. and K.S.) with more than 5 years of experience in CMR image post processing. All images were anonymized and read in a blinded fashion and a random order. Epi- and endocardial LV contours were manually traced on SSFP and Turbo-FLASH images. The papillary muscles and trabeculations were considered part of the LV cavity and were excluded from LV mass calculation (Fig. 1) [17]. To avoid any bias due to windowing, a default auto-windowing setting (type I) defined by the software was used for all images for visual assessment.

Visual assessment by an experienced physician is considered the gold standard for scar evaluation [17, 18]. Areas with delayed enhancement were manually traced for each slice. Areas of microvascular obstruction were manually traced and included in the total LGE mass. Results were reported as the percentage of LGE mass to the total myocardial LV mass. In addition to manual thresholding, we also measured the scar burden using a semi-automated thresholding method. Based on our experience and as reported by others [17], thresholds of 2SD and 3SD may overestimate LGE mass, and 5SD may underestimate the LGE mass. Therefore, we applied a threshold of 4SD above the mean SI of the normal remote myocardium on the SSFP and Turbo-FLASH LGE images with the previously drawn epi- and endocardial LV contours. A region of interest of visually normal remote myocardium was drawn for each slice. Subgroup analysis was performed to compare the LGE% between the two contrast agents in subjects with and without scar. Scar-positive subjects were also divided into two groups of ischemic and non-ischemic scar, and LGE% was compared between these two subgroups as well.

Qualitative analysis of scar burden

Two experienced physicians with 8 (A.R.G.) and 15 (M.L.S.) years of experience in diagnostic imaging independently performed blinded qualitative analysis. All images were anonymized, and all readings were performed in a random order. For both SSFP and Turbo-FLASH images, reader confidence in visualizing myocardial scar tissue was recorded on a 5-point scale for each CMR study (1 = poor, 2 = fair, 3 = good, 4 = very good, 5 = excellent). Hyper-enhanced

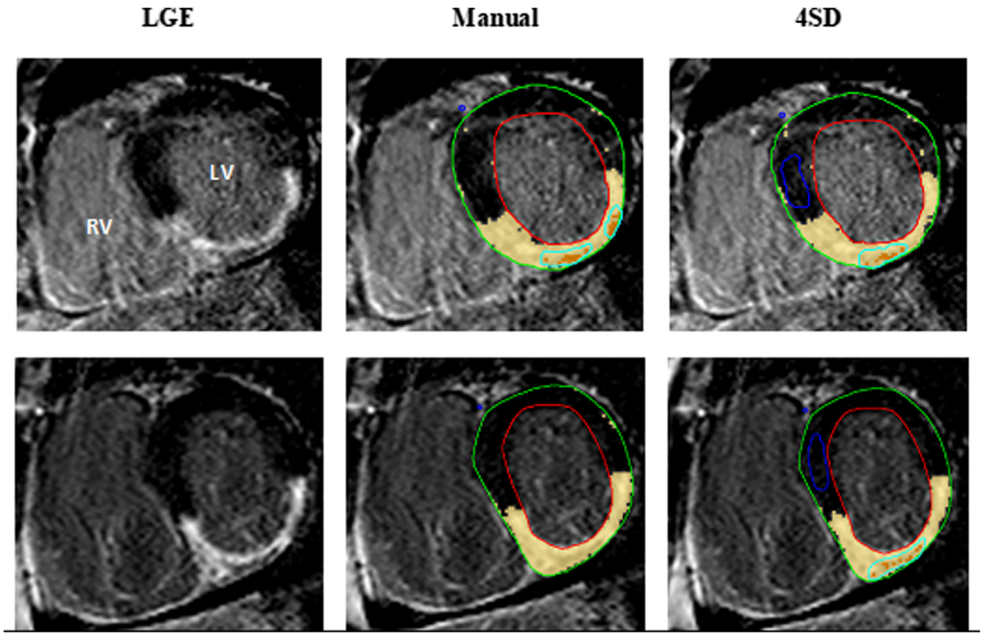

Fig. 1 Short-axis PSIR Turbo-FLASH images of a patient with myocardial infarction using gadobutrol (top) and gadoterate meglumine (bottom) performed 8 weeks apart. For each slice, epicardial (green) and endocardial (red) myocardial contours were delineated manually. Scar measurements were performed using two methods of (1) manual of raw late gadolinium-enhanced (LGE) area tracing and (2) thresholds of 4SD above the mean signal intensity of the normal remote myocardium (blue contours). Areas with microvascular obstruction, characterized by dense scarring with complete vascular blockage, were included manually (cyan contours)

myocardial scar area was qualitatively scored using the 16-segment AHA model based on the percent area (size) of scar per segment (0 = none, 1 = 1–25%, 2 = 26–50%, 3 = 51–75%, 4 = 76–100%). Segmental ratings were summed across all 16 segments to derive a global scar score for each scan (maximum possible score, 64) [1]. Additionally, the hyper-enhanced myocardial scar regions within the segment were also classified based on the scar location (no lesion, sub-endocardial, mid-myocardial, sub-epicardial, and transmural). Qualitative ratings for both readers were averaged and then compared between first and second scans.

LV scar/blood pool enhancement ratio

Parallel imaging with GRAPPA was used for image reconstruction during SSFP and Turbo-FLASH image acquisition. In parallel imaging with GRAPPA, noise does not follow a normal distribution function and varies spatially, resulting in inaccurate signal-to-noise (SNR) ratio values [19]. As an alternative method, we measured the LV blood pool and post-contrast scar tissue SI in both SSFP and Turbo-FLASH images. A ratio of scar enhancement was then calculated as [(LV blood pool SI − post-contrast scar SI)/(LV blood pool SI)]. This ratio was compared between the scans with gadobutrol and gadoterate meglumine as a surrogate of enhancement ratio induced by each contrast agent.

T1 and ECV measurements

Epi- and endocardial LV contours in the base, mid, and apical slices were manually delineated in the pre- and post-contrast T1 maps using Circle version 5.3. Additionally, pre- and post-contrast regions of interest were drawn in the LV blood pool cavity (excluding papillary muscles) for each of the three slices. Based on the 16-segment AHA model [20], pre- and post-contrast T1 values were determined and ECV was subsequently calculated using the following equation [8]: $ECV = (\Delta[1/T1myo]/\Delta[1/T1blood]) \times [1\text{-hematocrit}])$. Global ECV was calculated as the average of all 16 segmental ECV values. Segments demonstrating LGE were excluded from the averaged ECV value as previously recommended [21].

Statistical analysis

Continuous and categorical variables were expressed as means ± SD and numbers (%), respectively. Qualitative ratings were expressed as median (interquartile range [IQ]). Intraclass correlation coefficients (ICC) and their 95% confidence interval (CI) were calculated using two-way mixed-effect models to evaluate absolute agreement of LGE% and ECV between both CMR examinations. An ICC >0.8 was considered an excellent agreement. Bland–Altman plots were also performed to compare the quantitative measures. Inter- and intra-observer variability of LGE% and ECV measurement was evaluated using ICC for 16 randomly selected scans (8 baselines and 8 follow-ups). Paired *t* tests and Wilcoxon signed-rank tests were used to compare normally and non-normally distributed data between two scans, respectively. *P* values <0.05 were considered statistically significant. Statistical analysis was performed using SPSS 16 statistical software.

Results

All CMR examinations yielded diagnostic image quality. Patient characteristics and indication for CMR study are summarized in Table 1.

Scar measurements

Per the institutional imaging protocol for CMR, each CMR study can have both or either of SSFP or Turbo-FLASH

Table 1 Patient characteristics and indication for CMR study

Age (years)		61 ± 11
Male (%)		27 (67.5%)
Smoker (%)		2 (5%)
Diabetes mellitus (%)		5 (12.5%)
Hypertension (%)		32 (80%)
Dyslipidemia (%)		27 (67.5%)
Reason for CMR referral (%)	Suspected cardiomyopathy	15 (37.5%)
	Arrhythmia	6 (15%)
	AV disease or aortic dilation	15 (37.5%)
	Myopericarditis	3 (7.5%)
	Congenital cardiac disease	1 (2.5%)

Data are shown as mean ± SD for age and number (%) for the categorical variables. *AV* aortic valve, *CMR* cardiac magnetic resonance imaging

images. Of the 40 patients, 29 patients had Turbo-FLASH images on both first and second scans, and 36 had SSFP for both scans. Using the Turbo-FLASH technique and manual thresholding, LGE% was 9.9 ± 9.7% and 9.4 ± 9.7% for gadobutrol and gadoterate meglumine, respectively ($p = 0.232$) (ICC: 0.99, 95% CI: 0.97–0.99). Using a 4SD threshold, similar results were seen, with LGE% of 9.5 ± 9.7 and 9.2 ± 9.3 for gadobutrol and gadoterate meglumine, respectively ($p = 0.337$) (ICC: 0.98, 95% CI: 0.95–0.99). Using the SSFP technique and manual thresholding, LGE% averaged 7.5 ± 9.0% and 7.1 ± 8.6% for gadobutrol and gadoterate meglumine, respectively, using the SSFP technique ($p = 0.052$) (ICC: 0.99, 95% CI: 0.98–0.99). Again, for a 4SD threshold with the SSFP technique, comparable values were observed, with LGE% of 9.2 ± 8.5 and 8.87 ± 7.50 for gadobutrol and gadoterate meglumine, respectively ($p = 0.736$) (ICC: 0.98, 95% CI: 0.95–0.99) (Table 2, Fig. 2).

Additionally, by using Turbo-FLASH and SSFP techniques, the same analysis was performed in subjects with scar. The scar-positive subjects were stratified by ischemic versus non-ischemic scar. The analysis did not reveal any difference between the two contrast agents ($p > 0.05$) and the agreement remained excellent (Table 2). Segmental analysis using manual/4SD thresholding with either Turbo-Flash or SSFP techniques revealed no difference in LGE% measured between two contrast agents (Fig. 3).

Qualitative analysis

Reader confidence, and total scar score for Turbo-FLASH and SSFP images were assessed by both readers. For Turbo-FLASH images, the median (IQ) confidence rating for scar detection was 4.5 (4–5) for both gadobutrol and gadoterate meglumine. For SSFP images, the median (IQ) confidence rating for scar detection was 4.5 (4–5) for gadobutrol and 4 (4–5) for gadoterate meglumine. Median (IQ) summed segmental ratings for scar area with Turbo-FLASH images were 2 (0–9) and 2 (0–6.25) for gadobutrol and gadoterate meglumine, respectively ($p = 0.059$). With SSFP technique, median (IQ) summed segmental ratings for scar area were 1.25 (0–5) and 2 (0–7.25) for gadobutrol and gadoterate meglumine, respectively ($p = 0.781$).

Table 2 Level of agreement between gadobutrol and gadoterate meglumine for Turbo-FLASH and PSIR SSFP images using manual and 4SD thresholding methods

		Gadobutrol	Gadoterate meglumine	ICC (95% CI)
Turbo-FLASH (%) (all subjects)	Manual	9.9 ± 9.7	9.4 ± 9.7	0.99 (0.97–0.99)
	4SD	9.5 ± 9.7	9.2 ± 9.3	0.98 (0.95–0.99)
Turbo-FLASH (%) (scar + subjects)	Manual	12.8 ± 10.3	12.8 ± 10.1	0.99 (0.97–0.99)
	4SD	12.2 ± 10.9	12.3 ± 10	0.98 (0.94–0.99)
Turbo-FLASH (%) (ischemic scar)	Manual	14.7 ± 12.7	15.4 ± 11.4	0.98 (0.93–0.99)
	4SD	16.5 ± 12.3	17.1 ± 11.6	0.97 (0.87–0.99)
Turbo-FLASH (%) (non-ischemic scars)	Manual	11 ± 7.5	10.2 ± 8.3	0.99 (0.96–0.99)
	4SD	8.7 ± 8.7	8.4 ± 6.9	0.97 (0.89–0.99)
PSIR SSFP (%) (all subjects)	Manual	7.5 ± 9.0	7.1 ± 8.6	0.99 (0.98–0.99)
	4SD	9.2 ± 8.5	8.8 ± 7.5	0.98 (0.95–0.99)
PSIR SSFP (%) (scar + subjects)	Manual	11.2 ± 10.2	10.9 ± 9.6	0.99 (0.97–0.99)
	4SD	12.6 ± 9.8	11.7 ± 8.6	0.98 (0.94–0.99)
PSIR SSFP (%) (ischemic scars)	Manual	15.7 ± 12.9	15.5 ± 11.9	0.99 (0.97–0.99)
	4SD	16.7 ± 12.1	15.4 ± 11.2	0.99 (0.93–0.99)
PSIR SSFP (%) (non-ischemic scars)	Manual	7.2 ± 4.6	6.7 ± 4.1	0.96 (0.85–0.99)
	4SD	8.8 ± 5.2	8.5 ± 3.1	0.89 (0.57–0.97)
Myocardial native T1 (ms)		1004.2 ± 78	1017.2 ± 55	0.81 (0.47–0.93)
Blood pool native T1 (ms)		1633 ± 62	1647 ± 72	0.84 (0.54–0.95)
Myocardial CE T1 (ms)		361.7 ± 41	491.9 ± 47***	0.23 (− 0.07–0.64)
Blood pool CE T1 (ms)		230.5 ± 38.5	363.8 ± 52.2***	0.22 (− 0.08–0.63)
ECV (%)		28.40 ± 4.88	28.46 ± 4.73	0.98 (0.94–0.99)

CE contrast-enhanced, *ECV* extracellular volume, *ICC* intraclass correlation. Data are presented as mean ± SD. In this table, the difference and agreement between the two contrast agents have been evaluated using two different techniques of Turbo-FLASH and SSFP in all subjects (with and without scars), subjects with scar (ischemic and non-ischemic), subjects with only ischemic scars only, and subjects with non-ischemic scars. ***means $p < 0.001$

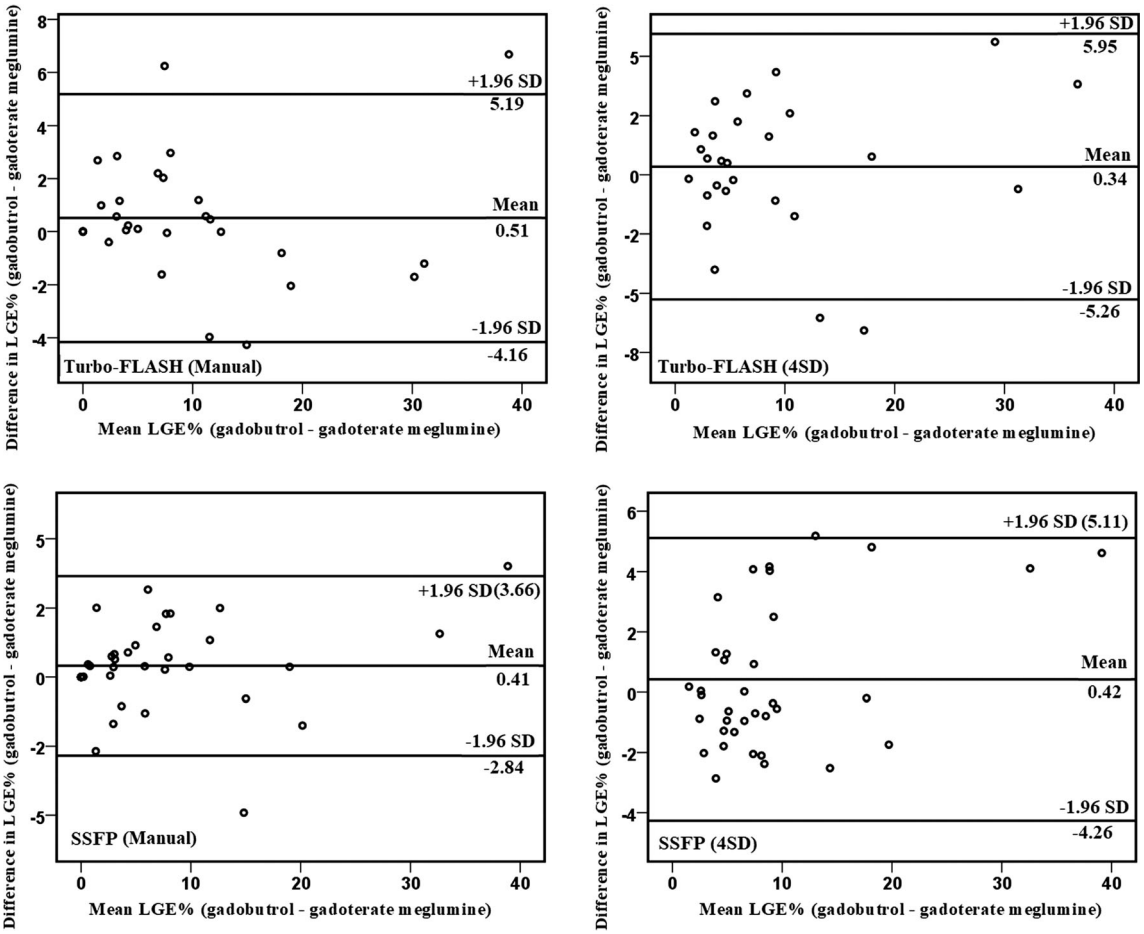

Fig. 2 LGE late gadolinium enhancement. In these Bland–Altman plots, results were shown as mean difference (lower limit of agreement, upper limit of agreement). Bland–Altman comparison of LGE% between gadobutrol and gadoterate meglumine. LGE% was compared between 2 contrast agents using PSIR Turbo-FLASH (top) and PSIR SSFP images (bottom). For each image, manual and 4SD thresholds were used to calculate LGE%

LV scar/blood pool enhancement ratio

The mean scar enhancement ratio for Turbo-FLASH images post-contrast injection was slightly higher in images acquired with gadobutrol vs. gadoterate meglumine (0.065 ± 0.086 vs. 0.057 ± 0.067), but this difference was not significantly different ($p = 0.462$). However, the scar enhancement ratios for SSFP images acquired post gadobutrol and gadoterate meglumine injection were 0.123 ± 0.087 and 0.098 ± 0.078, respectively, with a statistically significant difference between the two contrast agents ($p = 0.023$).

T1 and ECV measurements

Native and contrast-enhanced T1 values (myocardial and blood pool) and ECV values measured for both gadobutrol and gadoterate meglumine are shown in Table 2. Global native T1 values were comparable between the first and second scan; however, contrast-enhanced T1 values were significantly different ($p < 0.001$). Intraclass correlation between measured global ECV reached unity, and the values were highly comparable (Fig. 4). No difference in segmental analysis was observed between the two contrast agents for native T1 and ECV; however, contrast-enhanced T1 values were significantly different between the two contrast agents for all 16 segments ($p < 0.001$) (Fig. 5).

Inter- and intra-observer agreement

Sixteen scans (8 baselines and 8 follow-ups) were randomly selected. In addition to native-T1 and ECV values, measured scar percentage for SSFP and Turbo-FLASH images using manual and 4SD thresholding were obtained for each of the two readers. ICC showed excellent inter-observer and intra-observer agreement (data not shown).

Discussion

The purpose of this study was to compare the clinical performance of two macrocyclic contrast agents, gadobutrol and

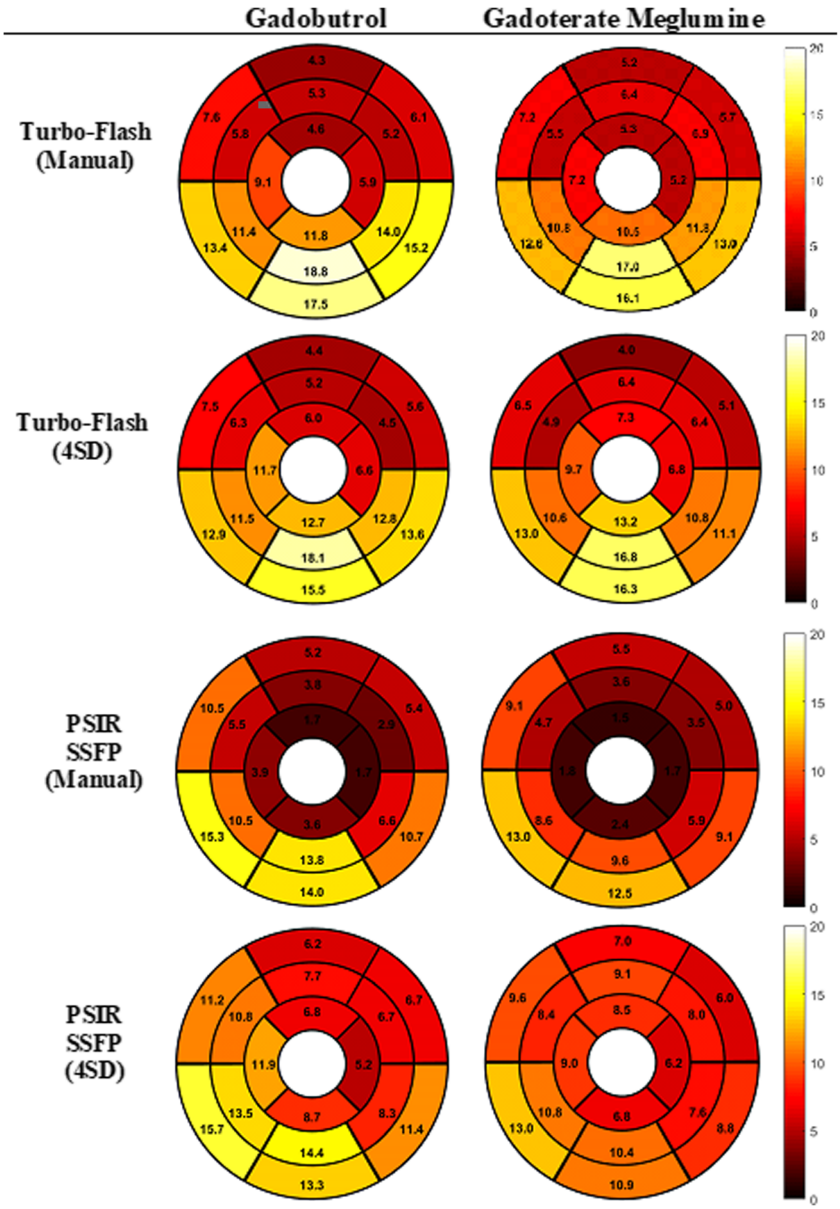

Fig. 3 Segmental LGE% measurements between two contrast agents using Turbo-Flash and SSFP images. No significant difference for any segments was observed for segmental analysis

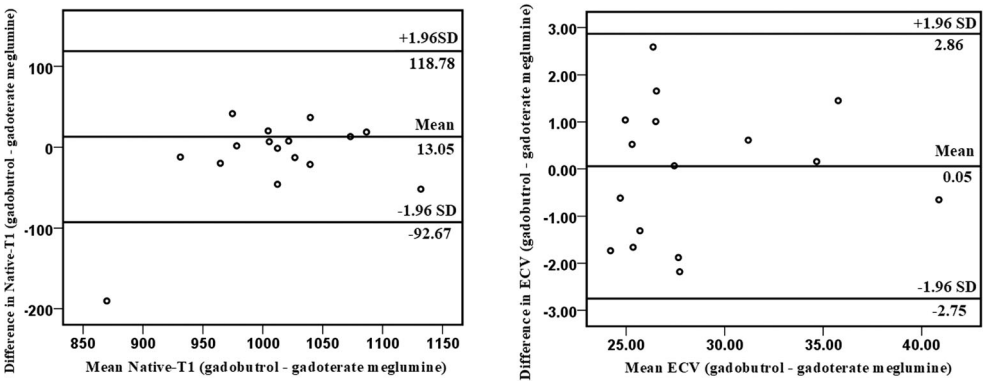

Fig. 4 ECV extracellular volume. In these Bland–Altman plots, results were shown as mean difference (lower limit of agreement, upper limit of agreement). Bland–Altman comparison of ECV between gadobutrol and gadoterate meglumine. Native T1 and ECV measurements using the gadobutrol and gadoterate meglumine

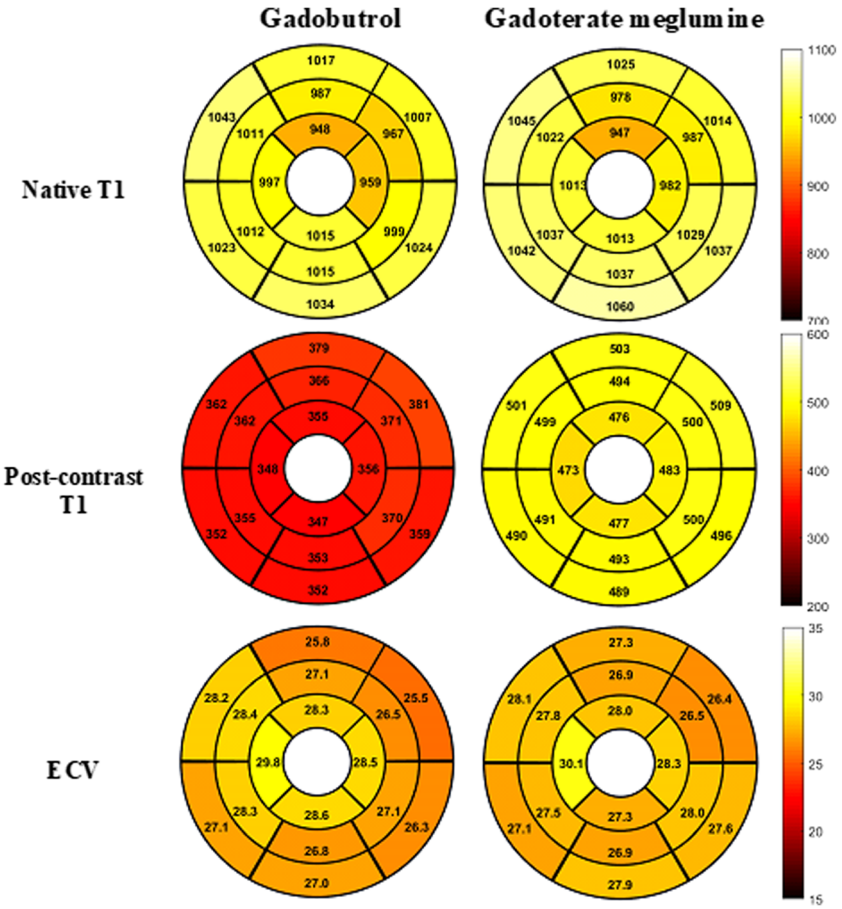

Fig. 5 Segmental native-, post-contrast T1, and ECV for gadobutrol and gadoterate meglumine. ECV extracellular volume fraction. No difference in segmental analysis was observed between two contrast agents for native T1 and ECV; however, contrast-enhanced T1 values were significantly different between the two contrast agents for all 16 segments ($p < 0.001$)

gadoterate meglumine, for LGE- and ECV-CMR imaging of patients with suspected cardiomyopathies. The measured LGE% was highly correlated between gadobutrol and gadoterate meglumine scans, which was confirmed by qualitative analysis. Both readers reported similar confidence scores to identify LGE between scans. Intraclass correlation for ECV calculation reached unity and the results revealed no difference between calculated ECV derived from the scan with either gadobutrol or gadoterate meglumine. Moreover, segmental analysis revealed no difference in LGE% and ECV measurements between two contrast agents.

Accurate detection of myocardial fibrosis by LGE-CMR is of high importance for risk stratification and therapy guidance in cardiomyopathy [22, 23]. Due to the high spatial resolution of CMR, small sub-endocardial lesions can be identified that might otherwise be missed by single-photon emission computed tomography (SPECT) [24]. To date, gadopentetate dimeglumine is the most widely studied and well-characterized GBCA [1–5, 22, 23]; however, a number of studies have shown that it may be associated with increased risk of gadolinium deposition independent of renal function [10–12]. Greater stability is particularly important in the setting of clinical CMR studies, where a double dose of contrast agent is the current standard of care for the identification of LGE lesions in patients with a GFR ≥ 60 mL/min/1.73 m^2. As patients undergoing CMR are exposed to higher concentrations of gadolinium in relation to other types of MR studies, the type of contrast agent selected (linear/macrocyclic) should be carefully considered. In the absence of longitudinal studies comparing linear and macrocyclic GBCAs or any clinical impact of gadolinium retention, migrating towards the use of contrast agents with a higher safety profile (like macrocyclic GBCAs) appears to be a reasonable precaution.

To our knowledge, only one study has compared LGE detection between gadobutrol and gadoterate meglumine. In that study [25], the efficacy of 0.15 mmol/kg gadobutrol was compared to a relaxivity-adjusted dose of gadoterate meglumine (0.22 mmol/kg) to measure LGE in 17 subjects with chronic myocardial infarction. In 14 subjects who had LGE, infarct sizes determined after administration of gadobutrol and gadoterate meglumine were not significantly different, in keeping with the findings of the present study. In clinical practice, the recommended dose of gadobutrol and gadoterate meglumine for adult and pediatric patients is 0.1 mmol/kg, but for CMR studies standard of care is to use 0.2 mmol/kg if GFR is ≥ 60 mL/min/1.73 m^2. Therefore, both CMR examinations in our study were performed using standard of care 0.2 mmol/kg gadobutrol and gadoterate meglumine. In addition, we

found lower LGE% using SSFP compared to Turbo-FLASH technique, which can be attributed to higher contrast-to-noise (CNR) and resolution with Turbo-FLASH compared to the SSFP technique, for differentiation of viable from nonviable myocardium as previously reported in patients with myocardial infarction [26].

High SNR and CNR ratios play a pivotal role in accurate determination of areas of scarring using LGE-CMR. Wagner et al [25] found that CNR between infarcted myocardium and remote myocardium did not differ significantly between gadobutrol vs. gadoterate meglumine. However, gadobutrol had greater contrast between infarcted myocardium and LV lumen in comparison with gadoterate meglumine. Because SNR measurements in parallel imaging with GRAPPA result in inaccurate values [19], SNR could not be conventionally measured in the current study. Instead, we calculated scar enhancement ratio between gadobutrol and gadoterate meglumine as an alternative: the difference between the LV blood pool SI and post-contrast scar SI divided by the LV blood pool SI. This ratio for Turbo-FLASH images post-contrast injection was slightly but not significantly higher in images acquired with gadobutrol vs. gadoterate meglumine. For SSFP images acquired with gadobutrol, this ratio was statistically higher in comparison with gadoterate meglumine. This difference in scar enhancement ratio explains why during qualitative evaluation of images, in some of the CMR studies performed with gadobutrol readers reported transmural scar while in the CMR examination done with gadoterate meglumine, subendocardial scar type was reported. This could be due to either overestimation of scar burden by gadobutrol or underestimation of scar burden by gadoterate meglumine. Our study was not designed to determine which agent is considered more accurate in the determination of scar burden. Further evaluation and correlation with animal studies (as a reference standard) is warranted to determine the correlation between the scar burden determined by pathology vs. scar burden visualized during CMR examination. This is important clinically in patients with ischemic heart disease as CMR can identify reversible vs. non-reversible myocardial lesions [5] and accurate identification of scar burden is crucial to decide whether patient will benefit from revascularization. In addition, we found that the right ventricular strain scars detected with gadobutrol were not observed in studies performed with gadoterate meglumine.

In our study, quantitative assessment of myocardial scar was performed on LGE-CMR data on short-axis images using manual thresholding and threshold of 4SD above the mean SI of the normal remote myocardium on the SSFP and Turbo-FLASH LGE images. The measured LGE% was highly correlated between gadobutrol and gadoterate meglumine scans using both techniques; however, confidence interval of manually traced LGE was narrower than that of 4SD-based semi-automatic measurement, both in Turbo-FLASH and SSFP. This difference is likely due to the fact that these semi-automated methods are highly dependent on the manual definition of remote (normal) myocardium [17] and thus may detect areas of LGE, which when assessed visually can be seen to represent artifact or noise. Moreover, the edges of the scar tissues such as gray zones play an important role in determination of scar mass. The 4SD thresholding technique tends to calculate a greater scar mass as it includes more of the gray zones than the manual approach. This is less prominent for Turbo-FLASH LGE images as they are less susceptible because of its higher spatial resolution and thus less gray zones.

T1 and ECV can be used to identify interstitial diffuse fibrosis and distinguish different disease processes [9]. Unlike native T1 relaxation times, contrast-enhanced T1 values are dependent and sensitive to the type of contrast agent, dosing, and renal clearance [7, 27]. On the other hand, ECV is a reproducible ratio derived from changes in pre- and post-contrast T1 relaxation times and is corrected for the hematocrit [21]. As expected, pre-contrast native T1 values were excellently associated intra-individually, but we observed significantly different contrast-enhanced T1 values. Results showed that contrast-enhanced T1 values were about 130 ms longer for gadoterate meglumine compared with gadobutrol. Lower post-contrast T1 with gadobutrol was likely due to higher relaxivity. Since post-contrast blood pool was also lower, ECV ratio remained the same, and we found a perfect correlation from the administration of the same dose of gadolinium injection from gadobutrol and gadoterate meglumine.

In a study by Kawel et al [28], authors found different intra-individual ECV values in 24 healthy subjects who underwent 3-T CMR using a bolus of 0.15 mmol/kg gadopentetate dimeglumine (Gd-DTPA; Magnevist) and 0.1 mmol/kg gadobenate dimeglumine (Gd-BOPTA; Multihance). The authors found that mean ECV values were slightly higher (by 1%, $p < 0.05$) for Gd-DTPA compared to Gd-BOPTA. However, this slight but significant difference could be secondary to the use of different doses of GBCA as they needed to be consistent with their institutional protocol. In addition, they found that following contrast injection, mean ECV increases linearly with time for both contrast agents [28]. In order to control for possible confounding variables between the two CMR examinations, we strictly matched the amount of gadolinium injected, image resolution, and time interval between contrast administration and image acquisition for SSFP, Turbo-FLASH, and MOLLI images.

Limitations

This study was subject to some limitations. First, we were not able to randomize patients to two groups, as patient enrollment occurred after undergoing the first CMR examination, which

was performed as part of the routine standard of care. Due to institutional policy, all clinical MR examinations had to be done by gadobutrol, so all patients received gadobutrol in the first CMR study and gadoterate meglumine in the second CMR research scan. Second, these two contrast agents may not have fully equivalent performance in identifying different types of scar (transmural, sub-endocardial, mid-myocardial, sub-epicardial). Since patients with different types of scar were enrolled in this study, subgroup analysis of scar tissues between two contrast agents for different scar types was not statistically powered to have a meaningful comparison. Third, although all the examinations were performed on 1.5-Tesla Siemens MR scanners, Avanto and Aera scanners were used during the first and second examinations respectively.

Conclusion

Our results indicate gadoterate meglumine has equivalent performance to gadobutrol in identifying LV myocardial scar at LGE-CMR qualitatively and quantitatively and can detect LGE with the same confidence level as gadobutrol. LGE- and ECV-CMR values derived from gadoterate meglumine were comparable with values derived from gadobutrol. Both macrocyclic GBCAs used in this study are well suited for CMR studies, with a lack of clinically relevant difference between gadobutrol and gadoterate meglumine and the contrast agents can be used interchangeably. Larger studies are warranted to explore the difference in scar classification and burden using different macrocyclic contrast agents.

Acknowledgements We would like to particularly thank all the patients who participated in our study.

Funding This study has received funding by Geurbet, LLC.

Compliance with ethical standards

Guarantor The scientific guarantor of this publication is Professor James C. Carr, MD.

Conflict of interest Dr. James Carr and Dr. Jeremy Collins are members of the advisory board of Guerbet, LLC.

Statistics and biometry No complex statistical methods were necessary for this paper.

Informed consent Written informed consent was obtained from all subjects (patients) in this study.

Ethical approval Institutional review board approval was obtained.

Methodology
- Prospective
- Diagnostic study
- Performed at one institution

References

1. Kino A, Zuehlsdorff S, Sheehan JJ et al (2009) Three-dimensional phase-sensitive inversion-recovery turbo FLASH sequence for the evaluation of left ventricular myocardial scar. AJR Am J Roentgenol 193(5):W381–W388
2. Kim RJ, Fieno DS, Parrish TB et al (1999) Relationship of MRI delayed contrast enhancement to irreversible injury, infarct age, and contractile function. Circulation 100(19):1992–2002
3. Schelbert EB, Hsu LY, Anderson SA et al (2010) Late gadolinium-enhancement cardiac magnetic resonance identifies postinfarction myocardial fibrosis and the border zone at the near cellular level in ex vivo rat heart. Circ Cardiovasc Imaging 3(6):743–752
4. Gulati A, Jabbour A, Ismail TF et al (2013) Association of fibrosis with mortality and sudden cardiac death in patients with nonischemic dilated cardiomyopathy. JAMA 309(9):896–908
5. Kim RJ, Wu E, Rafael A et al (2000) The use of contrast-enhanced magnetic resonance imaging to identify reversible myocardial dysfunction. N Engl J Med 343(20):1445–1453
6. Mewton N, Liu CY, Croisille P, Bluemke D, Lima JA (2011) Assessment of myocardial fibrosis with cardiovascular magnetic resonance. J Am Coll Cardiol 57(8):891–903
7. Ambale-Venkatesh B, Lima JA (2015) Cardiac MRI: a central prognostic tool in myocardial fibrosis. Nat Rev Cardiol 12(1):18–29
8. Kellman P, Wilson JR, Xue H, Ugander M, Arai AE (2012) Extracellular volume fraction mapping in the myocardium, part 1: evaluation of an automated method. J Cardiovasc Magn Reson 14: 63
9. Haaf P, Garg P, Messroghli DR, Broadbent DA, Greenwood JP, Plein S (2016) Cardiac T1 Mapping and Extracellular Volume (ECV) in clinical practice: a comprehensive review. J Cardiovasc Magn Reson 18(1):89
10. Errante Y, Cirimele V, Mallio CA, Di Lazzaro V, Zobel BB, Quattrocchi CC (2014) Progressive increase of T1 signal intensity of the dentate nucleus on unenhanced magnetic resonance images is associated with cumulative doses of intravenously administered gadodiamide in patients with normal renal function, suggesting dechelation. Invest Radiol 49(10):685–690
11. Kanda T, Ishii K, Kawaguchi H, Kitajima K, Takenaka D (2014) High signal intensity in the dentate nucleus and globus pallidus on unenhanced T1-weighted MR images: relationship with increasing cumulative dose of a gadolinium-based contrast material. Radiology 270(3):834–841
12. Kanda T, Osawa M, Oba H et al (2015) High signal intensity in dentate nucleus on unenhanced T1-weighted MR images: association with linear versus macrocyclic gadolinium chelate administration. Radiology 275(3):803–809
13. Idée JM, Port M, Robic C, Medina C, Sabatou M, Corot C (2009) Role of thermodynamic and kinetic parameters in gadolinium chelate stability. J Magn Reson Imaging 30(6):1249–1258
14. Kim RJ, Shah DJ, Judd RM (2003) How we perform delayed enhancement imaging. J Cardiovasc Magn Reson 5(3):505–514
15. Messroghli DR, Greiser A, Fröhlich M, Dietz R, Schulz-Menger J (2007) Optimization and validation of a fully-integrated pulse sequence for modified look-locker inversion-recovery (MOLLI) T1 mapping of the heart. J Magn Reson Imaging 26(4):1081–1086
16. Stirrat J, Joncas SX, Salerno M, Drangova M, White J (2015) Influence of phase correction of late gadolinium enhancement images on scar signal quantification in patients with ischemic and non-ischemic cardiomyopathy. J Cardiovasc Magn Reson 17:66
17. Vermes E, Childs H, Carbone I, Barckow P, Friedrich MG (2013) Auto-threshold quantification of late gadolinium enhancement in patients with acute heart disease. J Magn Reson Imaging 37(2): 382–390

18. Mikami Y, Kolman L, Joncas SX et al (2014) Accuracy and reproducibility of semi-automated late gadolinium enhancement quantification techniques in patients with hypertrophic cardiomyopathy. J Cardiovasc Magn Reson 16:85
19. Dietrich O, Raya JG, Reeder SB, Reiser MF, Schoenberg SO (2007) Measurement of signal-to-noise ratios in MR images: influence of multichannel coils, parallel imaging, and reconstruction filters. J Magn Reson Imaging 26(2):375–385
20. Cerqueira MD, Weissman NJ, Dilsizian V et al (2002) Standardized myocardial segmentation and nomenclature for tomographic imaging of the heart. A statement for healthcare professionals from the Cardiac Imaging Committee of the Council on Clinical Cardiology of the American Heart Association. Circulation 105(4):539–542
21. Moon JC, Messroghli DR, Kellman P et al (2013) Myocardial T1 mapping and extracellular volume quantification: a Society for Cardiovascular Magnetic Resonance (SCMR) and CMR Working Group of the European Society of cardiology consensus statement. J Cardiovasc Magn Reson 15:92
22. Assomull RG, Prasad SK, Lyne J et al (2006) Cardiovascular magnetic resonance, fibrosis, and prognosis in dilated cardiomyopathy. J Am Coll Cardiol 48(10):1977–1985
23. Bello D, Fieno DS, Kim RJ et al (2005) Infarct morphology identifies patients with substrate for sustained ventricular tachycardia. J Am Coll Cardiol 45(7):1104–1108
24. Wagner A, Mahrholdt H, Holly TA et al (2003) Contrast-enhanced MRI and routine single photon emission computed tomography (SPECT) perfusion imaging for detection of subendocardial myocardial infarcts: an imaging study. Lancet 361(9355):374–379
25. Wagner M, Schilling R, Doeblin P et al (2013) Macrocyclic contrast agents for magnetic resonance imaging of chronic myocardial infarction: intraindividual comparison of gadobutrol and gadoterate meglumine. Eur Radiol 23(1):108–114
26. Huber A, Schoenberg SO, Spannagl B et al (2006) Single-shot inversion recovery TrueFISP for assessment of myocardial infarction. AJR Am J Roentgenol 186(3):627–633
27. Gai N, Turkbey EB, Nazarian S et al (2011) T1 mapping of the gadolinium-enhanced myocardium: adjustment for factors affecting interpatient comparison. Magn Reson Med 65(5):1407–1415
28. Kawel N, Nacif M, Zavodni A et al (2012) T1 mapping of the myocardium: intra-individual assessment of post-contrast T1 time evolution and extracellular volume fraction at 3T for Gd-DTPA and Gd-BOPTA. J Cardiovasc Magn Reson 14:26